Antenna Array Absolute Self-Calibration and Application to Separate Tx/Rx Array Full Duplex MIMO

Kalyana Gopala, Dirk Slock
EURECOM, Sophia-Antipolis, France, Email: {gopala,slock}@eurecom.fr

***Abstract*—Full Duplex communication is one of the promising candidate technologies for 5G. As is well known, the key challenge is the mitigation of self interference at the receiver of the Full Duplex system from its own transmitter. With separate transmit (Tx) and Receive (Rx) antenna arrays, the transmitter can beamform in such a manner as to minimize the self interference. The number of constraints this poses on the Tx beamformer would be limited if the internal MIMO channel between Tx and Rx arrays would have limited rank. Hence, in this work, we focus on characterizing the internal channel between antenna subsets of an array. An impediment to the determination of the internal propagation channel is that the estimated (digital domain) channel also involves the impact of the Tx and Rx front ends. Hence, it becomes necessary to estimate these absolute (Tx and Rx) calibration parameters as well, for which we propose two approaches. In a first approach, we assume a parameterized path loss based model for the internal propagation channel and estimate in an alternating fashion the calibration and path loss parameters. In the second approach, we exploit the symmetry of the MIMO propagation channel and temporal variation of the calibration parameters to estimate all unknowns without any further model assumptions. We provide a measurement based comparison between the different estimation approaches and apply the calibration to exhibit the singular value profile of full duplex MIMO internal propagation channels in our testbed. The proposed absolute self-calibration has, of course, many other applications such as for the antenna array manifold in Direction-of-Arrival (DoA) estimation and DoA based beamforming.**

I. Introduction

5th generation wireless systems (5G) promises 1000 fold improvement in the system capacity. This increase comes from multiple advances like densification of the cells, Massive number of antennas (Massive MIMO), moving to mm Wave frequencies, paradigms like Licensed Shared Access (LSA) to reuse the existing spectrum, etc. Another key contender is Full Duplex communication, which can potentially double the network capacity, or much more [1]. Legacy communication systems either transmit (Tx) or receive (Rx) at a given time using a given frequency. Full Duplex (FD) communication proposes to have simultaneous Tx and Rx at the same frequency and at the same time instant. Of course, this results in severe self interference at the receiver of the FD system from its own transmitter. For a proper reception, 80-120dB of self interference mitigation is called for. Several works [2], [3] have demonstrated that this can indeed be achieved by a necessary combination of multiple techniques - antenna, RF, analog and digital. A simple instance is to isolate the transmit and receive antennas to increase the attenuation from the Tx to the Rx antenna. With the advent of multiple antennas, another approach is to beamform from the Tx in such a manner as to minimize the self interference at the Rx antennas. [4], [5] propose a 2x2 Full Duplex MIMO system where the beamforming weights are adjusted to selectively cancel the Tx signal at the Rx'r. [6] experimentally shows the feasibility of this approach for a 72 element antenna array. As concerns the multiple antenna beamforming, the lower the number of significant singular values in the channel between the antennas of the Tx and Rx, the lesser the number of Tx antennas required to create nulls at the Rx antennas. Thus, the MIMO self-interference channel that we investigate here is strongly dependent on the antenna arrays involved and can be optimized to reach a desirable rank profile behavior. The channel, as it is measured in the digital domain, depends of course, on the propagation channel, but also depends on the absolute calibration factors of the Tx and Rx RF chains, of which strong variation over antennas may significantly influence the measured MIMO channel singular value profile. In order to make sure that the conclusions that we draw about this profile are due to the antenna arrays only, and not the particular RF equipment used, we extract the propagation channel from the digital channel by absolute calibration in order to investigate its RF independent profile. Hence, in this work, we focus on estimating the internal channel across the antennas of an antenna array, in particular across the antennas of a Massive MIMO array (Figure 1) that is part of the Open Air Interface (OAI) [7] platform at Eurecom.

Note that related issues typically arise in channel reciprocity calibration for TDD (Time Division Duplexing) multiple antenna systems where, however, one only needs the ratio of the Tx and Rx calibration factors, called the relative calibration factor [8]. However, here we are interested in the explicit computation of the internal propagation channel, hence it becomes necessary to estimate the absolute calibration parameters as well. Several original approaches are proposed in this paper for the estimation of these parameters. The proposed calibration techniques are blind, in contrast to classical absolute calibration which requires extra measurement equipment [9], hence the term "self calibration". The proposed techniques all lead to cost functions that are optimized by alternating

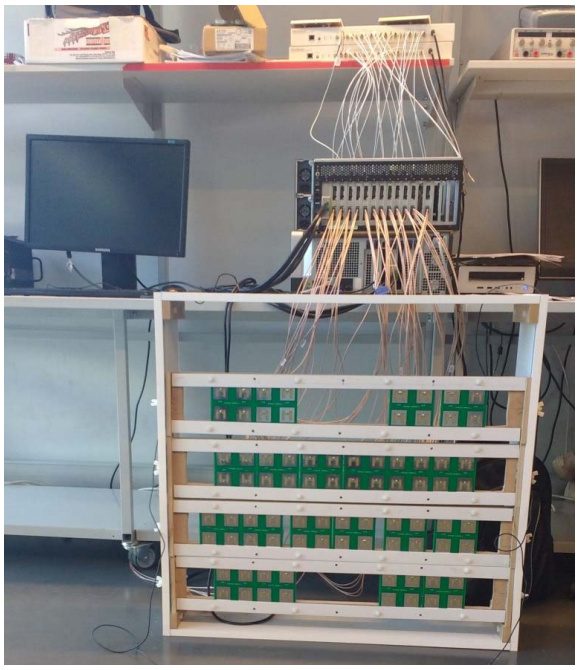

Fig. 1. Eurecom Massive MIMO antenna array with 48 antennas

minimization which guarantees convergence. Note that the absolute calibration factors are of interest in their own right as they are also needed in the determination of the antenna array response for Direction-of-Arrival (DoA) estimation or DoA based beamforming. The particular singular value profiles of the internal MIMO channels measured and presented here do of course depend on the particular antennas and Tx/Rx antenna array configurations employed. Hence multiple subarrays of a Massive MIMO array are considered here. But at least the dependence on the RF equipment gets eliminated by the absolute calibration.

In section II, we describe the system model that we use from where the internal propagation channel is estimated. The different estimation algorithms for the internal propagation channel are given in sections III and IV. In section V, we describe the Eurecom Massive MIMO antenna array and the framework for the internal channel measurement. The proposed algorithms are then used to estimate the internal propagation channel of the OAI Massive MIMO antenna array and the results are elaborated in section VI. Finally, some conclusions are given in section VII.

II. System Model

Let $\mathbf{H}$ be the measured channel matrix across the antennas, where $\mathbf{H}_{ij}$ is the measured channel from transmit antenna j to receive antenna i. Then

$$\mathbf{H} = \mathbf{RCT} + \mathbf{V}, \tag{1}$$

where $\mathbf{R}$ and $\mathbf{T}$ are diagonal matrices corresponding to the receive and transmit calibration parameters respectively. Prior measurement campaigns [10], [11] have shown that the calibration matrices are diagonal (up to at least -30dB). We shall assume diagonal matrices for the absolute calibration factors because the targeted application here is just to compensate (approximately) for the RF circuitry in the investigation of the singular value profile of a MIMO intra-array channel. Note that $\mathbf{C}$ is the intra-array propagation channel that we are interested in estimating and $\mathbf{V}$ accounts for the measurement noise. In this publication, we restrict our attention to determining the intra-array propagation channel (also called the internal propagation channel or just internal channel in short) corresponding to just one or two rows of the overall antenna array. A more detailed publication giving the results of the intra-array channel across the entire antenna array is in the works. Note that in the estimation of the internal channel, there is always a complex scale ambiguity that cannot be resolved as the unknowns $\mathbf{R}$, $\mathbf{C}$ and $\mathbf{T}$ appear in a multiplicative fashion. However, this is is not crucial as our interest is in studying the singular value profile of the internal propagation channel matrix. Note that this propagation channel will, of course, depend on the particular antenna array, but we are able to remove the effect of the RF units.

III. Estimation assuming a pathloss propagation channel model

In this approach, we model the internal channel with a simple path loss model where the channel amplitude and phase are functions of the distance between the antennas in question.The distance between the antennas (and thus, in general, the geometry) is assumed to be known for this method.

A. Estimation of Magnitude of the internal channel

Here, we focus only on estimating the magnitude of the internal channel. We begin with a model for the internal propagation channel and iteratively compute the path loss exponent of this internal channel as well as the magnitude of the diagonal matrices $\mathbf{R}$, $\mathbf{T}$. Thus, we assume a pathloss model for the internal matrix,

$$\bar{\mathbf{C}}_{ij} = \frac{\alpha}{d_{ij}^{\gamma}}. \tag{2}$$

Here, the overbar notation on a matrix corresponds to the magnitude of the elements of that matrix. α is an unknown constant, γ is an exponent in the pathloss factor that needs to be determined, d_{ij} are the measured distances between antennas i, j on the physical antenna array. Taking the magnitude on both sides of equation (1), and ignoring the noise, we get

$$\bar{\mathbf{H}} = \bar{\mathbf{R}}\bar{\mathbf{C}}\bar{\mathbf{T}}. \tag{3}$$

Vectorizing the above, we get,

$$\text{vec}(\bar{\mathbf{H}}) = (\mathbf{I} * \bar{\mathbf{R}}\bar{\mathbf{C}})\bar{\mathbf{t}}, \tag{4}$$

where $\bar{\mathbf{t}} = \text{diag}\,(\bar{\mathbf{T}})$ and $*$ denotes the Khatri–Rao product, [12], which is the column-wise Kronecker product. With matrices $\mathbf{A}$ and $\mathbf{B}$ partitioned into columns, $\mathbf{A} = \begin{bmatrix}\mathbf{a}_1 & \mathbf{a}_2 & \dots & \mathbf{a}_M\end{bmatrix}$ and $\mathbf{B} = \begin{bmatrix}\mathbf{b}_1 & \mathbf{b}_2 & \dots & \mathbf{b}_M\end{bmatrix}$ where $\mathbf{a}_i$ and $\mathbf{b}_i$ are column vectors for $i \in 1 \cdots M$,

$$\mathbf{A} * \mathbf{B} = \begin{bmatrix}\mathbf{a}_1 \otimes \mathbf{b}_1 & \mathbf{a}_2 \otimes \mathbf{b}_2 & \dots & \mathbf{a}_M \otimes \mathbf{b}_M\end{bmatrix}.$$

To arrive at (4), we have used the property $\text{vec}(\mathbf{A}\ \text{diag}\,(\mathbf{x})\,\mathbf{B}) = (\mathbf{B^T} * \mathbf{A})\,\mathbf{x}$. The notation $\text{diag}\,(\mathbf{x})$ refers to a diagonal matrix whose diagonal elements are formed out of the vector $\mathbf{x}$. With this formulation, we get $N^2 - N$ equations for $2N$ unknowns ($2N-1$ unknowns in $\mathbf{R}$,$\mathbf{T}$ and an unknown γ). Note that the number of equations is $N^2 - N$ as the diagonal elements of the channel matrices cannot be used. Then, the least squares solution for $\bar{\mathbf{t}}$ may be determined as,

$$\bar{\mathbf{t}} = (\mathbf{A}^H\mathbf{A})^{-1}\mathbf{A}^H\text{vec}(\bar{\mathbf{H}}),\ \mathbf{A} = (\mathbf{I} * \bar{\mathbf{R}}\bar{\mathbf{C}}) \tag{7}$$

Similarly, $\bar{\mathbf{R}}$ may be estimated once $\bar{\mathbf{T}}$ is known. For every value of $\bar{\mathbf{R}}$ and $\bar{\mathbf{T}}$, the value of γ is derived using an exhaustive search over the range of values $1-2$ in step size of 0.01. The overall algorithm can thus be summarized as in Table I.

TABLE I
OVERALL ALGORITHM TO DETERMINE THE INTERNAL CHANNEL PARAMETERS USING ONLY THE MAGNITUDE INFORMATION.

Initialize $\bar{\mathbf{R}} = \mathbf{I}$.
Initialize $\bar{\mathbf{C}}$ according to (2) with $\gamma = 1$.Choose $\alpha = 1$.
Repeat until convergence
Update Tx calibration matrix
$\bar{\mathbf{t}} = (\mathbf{A}^H\mathbf{A})^{-1}\mathbf{A}^H\text{vec}(\bar{\mathbf{H}}),\ \mathbf{A} = (\mathbf{I} * \bar{\mathbf{R}}\bar{\mathbf{C}})$
$\bar{\mathbf{T}} = \text{diag}\,(\bar{\mathbf{t}})$
Update Rx calibration matrix
$\bar{\mathbf{r}} = (\mathbf{B}^H\mathbf{B})^{-1}\mathbf{B}^H\text{vec}(\bar{\mathbf{H}}^T),\ \mathbf{B} = (\mathbf{I} * \bar{\mathbf{T}}\bar{\mathbf{C}})$
$\bar{\mathbf{R}} = \text{diag}\,(\bar{\mathbf{r}})$
Update pathloss scale factor
for γ_1 = 1:0.01:2
$\bar{\mathbf{C}}_{ij} = \frac{\alpha}{d_{ij}^{\gamma_1}}$.
LSE(γ_1) = $||\text{vec}(\bar{\mathbf{H}}) - (\mathbf{I} * \bar{\mathbf{R}}\bar{\mathbf{C}})\bar{\mathbf{t}}||^2$
$\gamma = \min_{\gamma_1}$ LSE

B. Estimation of Magnitude and Phase of the internal channel

Here, we estimate both the magnitude and phase of the internal channel. The matrix $\mathbf{C}$ is hence modeled as,

$$\mathbf{C}_{i\to j} = \frac{\alpha}{d_{ij}^{\gamma}}\mathbf{e}^{\mathbf{j}2\pi\frac{\mathbf{f_c}}{\mathbf{c}}\mathbf{d_{ij}}} \tag{8}$$

where α is an unknown constant and γ is the pathloss exponent to be determined. $c = 3e8m/s$, the velocity of light.

This can, in turn, be used to solve for $\mathbf{R}$ and $\mathbf{T}$ using alternating optimization. Given $\mathbf{R}$, as seen before in III-A,

$$\text{vec}(\mathbf{H}) = (\mathbf{I} * \mathbf{RC})\mathbf{t}, \tag{9}$$

where $\mathbf{t} = \text{diag}\,(\mathbf{T})$. Then, the least squares solution for $\mathbf{t}$ is given as,

$$\mathbf{t} = (\mathbf{A}^H\mathbf{A})^{-1}\mathbf{A}^H\text{vec}(\mathbf{H}),\ \mathbf{A} = (\mathbf{I} * \mathbf{RC}) \tag{10}$$

The overall algorithm can thus be summarized as in section III-A, but we omit explicitly writing it down due to space constraints. To generalize this further, suppose we model the internal channel as

$$\mathbf{C}_{i\to j} = \frac{\alpha}{d_{ij}^{\gamma}}\mathbf{e}^{\mathbf{j}\beta\mathbf{d_{ij}}} \tag{11}$$

where $\beta \in [0, 20\pi)$, instead of as in (8). We can then perform a computation of the additional parameter β too in an alternating minimization fashion along with $\mathbf{R}$, $\mathbf{T}$ and the pathloss exponent γ. The β is determined by performing an exhaustive search over the range $[0, 20\pi)$. The upper limit for β is arbitrary and chosen to include the value $2\pi\frac{f_c}{c}$ that is used in the distance dependent phase assumption.

IV. DIRECT ESTIMATION OF THE PROPAGATION CHANNEL

In this approach, instead of assuming a model for the internal channel, we directly estimate $\mathbf{C}$. We exploit the fact that the internal channel matrix $\mathbf{C}$ is symmetric. If we observe (1), there are 3 sets of unknowns $\mathbf{R}$, $\mathbf{C}$, and $\mathbf{T}$ to be determined. Since the product of the three appears, two scale factor ambiguities appear also. The number of equations available is $N^2 - N$ whereas the number of unknowns would be $2N - 2 + \frac{N^2-N}{2}$ (namely $2N$ for the calibration parameters, $\frac{N^2-N}{2}$ for the internal channel, minus 2 for the two scale factor ambiguities). By comparing the numbers of unknowns and equations, we get identifiability whenever $N \geq 4$.

To further improve the estimation, we exploit the fact that the internal channel $\mathbf{C}$ stays constant except for the possible presence of relatively weak multipath (particularly when the Tx/Rx arrays being considered are not very far apart). On the other hand, each time the hardware setup is restarted, the absolute calibration factors $\mathbf{R}$ and $\mathbf{T}$ take new independent values. Hence, every channel measurement upon resetting the hardware can result in a completely independent set of equations. In this new set of equations, of course, the $\mathbf{R}$ and $\mathbf{T}$ bring in new sets of unknowns but the internal propagation channel $\mathbf{C}$ remains constant. Upon accumulating these observations, we would have an over-determined set of equations for the internal channel $\mathbf{C}$. Stacking l such independent observations of the measured channel, we get

$$\begin{aligned}\mathbf{H}_1 &= \mathbf{R}_1\mathbf{C}\mathbf{T}_1 + \mathbf{V}_1\\ \mathbf{H}_2 &= \mathbf{R}_2\mathbf{C}\mathbf{T}_2 + \mathbf{V}_2\\ &\vdots\\ \mathbf{H}_l &= \mathbf{R}_l\mathbf{C}\mathbf{T}_l + \mathbf{V}_l\end{aligned} \tag{12}$$

To solve this, we follow the alternating minimization approach as in III, except that now the internal propagation channel $\mathbf{C}$ also has to be estimated. To estimate the transmit calibration parameters $\mathbf{t}$, the following formulation may be used.

$$\underbrace{\begin{bmatrix}\text{vec}(\mathbf{H}_1)\\ \text{vec}(\mathbf{H}_2)\\ \vdots\\ \text{vec}(\mathbf{H}_l)\end{bmatrix}}_{\mathbb{H}} = \underbrace{\begin{bmatrix}\mathbf{I} * \mathbf{R}_1\mathbf{C}\\ \mathbf{I} * \mathbf{R}_2\mathbf{C}\\ \vdots\\ \mathbf{I} * \mathbf{R}_l\mathbf{C}\end{bmatrix}}_{\mathbf{A}}\mathbf{t} + \begin{bmatrix}\text{vec}(\mathbf{V}_1)\\ \text{vec}(\mathbf{V}_2)\\ \vdots\\ \text{vec}(\mathbf{V}_l)\end{bmatrix} \tag{13}$$

Similarly, the following formulation may be used to derive the

TABLE II
OVERALL ALGORITHM TO ESTIMATE INTERNAL CHANNEL VALUES DIRECTLY.

Choose $\alpha = 1$. Initialize $\mathbf{R} = \mathbf{I}$,
$\mathbf{C}$ a symmetric Toeplitz matrix with first colum [0 1 0 ...]
Repeat until convergence
Update Tx calibration matrix
$\mathbf{t} = (\mathbf{A}^H\mathbf{A})^{-1}\mathbf{A}^H\mathbb{H}$, see (13)
$\mathbf{T} = \text{diag}(\mathbf{t})$
Update Rx calibration matrix
$\mathbf{r} = (\mathbf{B}^H\mathbf{B})^{-1}\mathbf{B}^H\mathcal{H}$, see (14)
$\mathbf{R} = \text{diag}(\mathbf{r})$
Update Internal propagation matrix
$\mathbf{c} = (\mathbf{Q}^H\mathbf{Q})^{-1}\mathbf{Q}^H\mathbb{H}$, see (13)
LSE $= \|\|\mathbb{H} - \mathbf{Qc}\|\|^2$

receive calibration parameters $\mathbf{r}$.

$$\underbrace{\begin{bmatrix}\text{vec}(\mathbf{H}_1^T)\\ \text{vec}(\mathbf{H}_2^T)\\ \vdots \\ \text{vec}(\mathbf{H}_l^T)\end{bmatrix}}_{\mathcal{H}} = \underbrace{\begin{bmatrix}\mathbf{I} * \mathbf{T}_1\mathbf{C}\\ \mathbf{I} * \mathbf{T}_2\mathbf{C}\\ \vdots \\ \mathbf{I} * \mathbf{T}_l\mathbf{C}\end{bmatrix}}_{\mathbf{B}} \mathbf{r} + \begin{bmatrix}\text{vec}(\mathbf{V}_1^T)\\ \text{vec}(\mathbf{V}_2^T)\\ \vdots \\ \text{vec}(\mathbf{V}_l^T)\end{bmatrix} \tag{14}$$

Remains now to determine the propagation channel $\mathbf{C}$.

$$\underbrace{\begin{bmatrix}\text{vec}(\mathbf{H}_1)\\ \text{vec}(\mathbf{H}_2)\\ \vdots \\ \text{vec}(\mathbf{H}_l)\end{bmatrix}}_{\mathbb{H}} = \underbrace{\begin{bmatrix}\mathbf{T}_1 \otimes \mathbf{R}_1\\ \mathbf{T}_2 \otimes \mathbf{R}_2\\ \vdots \\ \mathbf{T}_l \otimes \mathbf{R}_l\end{bmatrix}}_{\mathbf{Q}'} \text{vec}(\mathbf{C}) + \begin{bmatrix}\text{vec}(\mathbf{V}_1)\\ \text{vec}(\mathbf{V}_2)\\ \vdots \\ \text{vec}(\mathbf{V}_l)\end{bmatrix} \tag{15}$$

Noting that $\mathbf{C}$ is a symmetric matrix, the elements in the lower triangular portion of $\mathbf{C}$ are the same as that in the upper triangular portion. Let the vector of these elements in the lower triangular portion be denoted as $\mathbf{c}$. Then, (15) may be rewritten as,

$$\underbrace{\begin{bmatrix}\text{vec}(\mathbf{H}_1)\\ \text{vec}(\mathbf{H}_2)\\ \vdots \\ \text{vec}(\mathbf{H}_l)\end{bmatrix}}_{\mathbb{H}} = \mathbf{Q}\,\mathbf{c} + \begin{bmatrix}\text{vec}(\mathbf{V}_1)\\ \text{vec}(\mathbf{V}_2)\\ \vdots \\ \text{vec}(\mathbf{V}_l)\end{bmatrix} \tag{16}$$

where $\mathbf{Q}$ is a reduced matrix obtained by merging the columns in $\mathbf{Q}'$ that correspond to the same entry of $\mathbf{C}$. The overall algorithm is given in Table II.

V. MEASUREMENT SETUP

The Eurecom Massive MIMO array (Figure 1) is constructed with several microstrip antenna cards. Each such microstrip card, in turn, has 4 antennas. Figure 2 shows the 48 connected antennas (in green) amongst these cards. The rest of the antennas are unconnected. The 48 antennas are driven by 12 radio cards, where each radio card has 4 transceiver units. The transmission happens at carrier frequency $f_c = 2.66$GHz and the sampling frequency $f_s = 7.68$MHz corresponding to a 5MHz LTE transmission. Figure 2 also shows the numbering of the antennas in pairs where the first value corresponds to the radio card index and the next is the relative numbering within the radio card. For instance (10,3) would correspond to the antenna index $10 \times 4 + 3 = 43$, where the antenna numbering starts from 0. In the same figure, the dimensions of the cards are also given to enable the calculation of the distances between antennas.

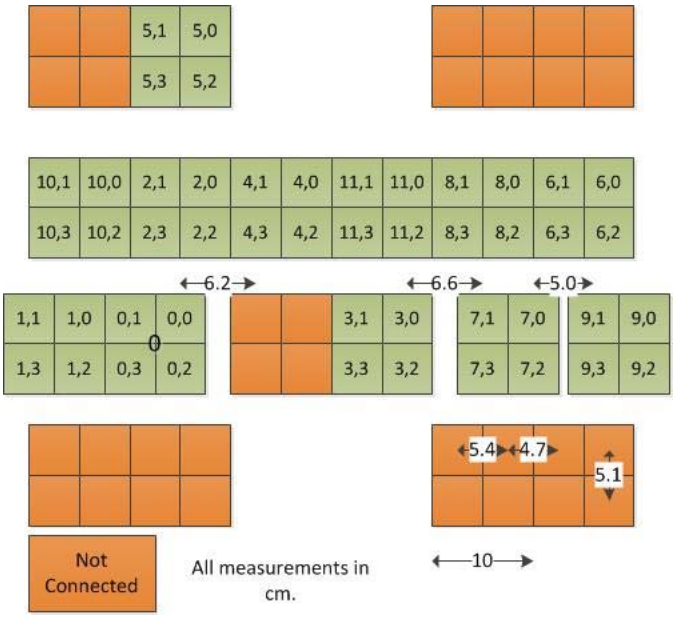

Fig. 2. Numbering of the antennas in the Massive MIMO array

Thus, if we consider row 3 (counting from the top row as 1) in Figure 2, the measured channel $\mathbf{H}$ would be a matrix of dimension 12×12. The diagonal elements of this matrix would be zero. The first super (or sub) diagonal of this matrix corresponds to the channel between the adjacent antennas. Similarly, the second super (or sub) diagonal corresponds to the measurements across alternate antennas and so on. While comparing the performance of the various estimation algorithms, the focus is on the channel estimation of row 3. It must also be noted that the directivity of the antennas is perpendicular to the plane of the antennas and hence the internal propagation channel is attenuated by design in the plane of the antennas which aids in the self interference cancellation by providing a kind of isolation between the antenna elements. It should also be noted that on row 3, the antennas are not equispaced. The distance between antennas alternates between 5.4cm and 4.7cm.

A. Frame structure for internal calibration

The Massive MIMO array is enabled by Eurecom's OAI platform. Among other things, it also enables the transmission of a 10 ms Long term evolution (LTE) like OFDM (Orthogonal Frequency Division Multiplexing) frame. As the transmission is happening in a controlled environment, every subcarrier of this frame may be treated like a pilot for channel estimation.

To ensure channel coherence, the measurement of the channels need to be done as quickly as possible. Hence, we attempt to complete channel measurements across all the antennas within one OFDM frame of 10ms. In LTE, an OFDM frame has 120 OFDM symbols. As we have 48 antennas, this implies that we can only allocate 2 OFDM symbols per antenna if all the antennas have to finish transmission during one OFDM frame. Thus, every antenna transmits in a round robin fashion for two OFDM symbols. During the last 24 OFDM symbols, all the antennas are in receive mode. The frame structure is shown in Figure 3. The estimated digital channel for every antenna is averaged over the two OFDM symbols to obtain **H**.

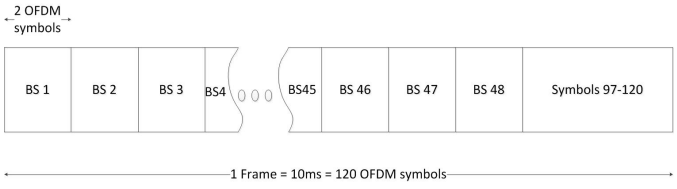

Fig. 3. The frame used to estimate the channel across all the BSs. Each BS transmits during the allocated symbols and reverts to receive mode during all the other symbols.

VI. Experimental Results

A. Absolute Self-Calibration

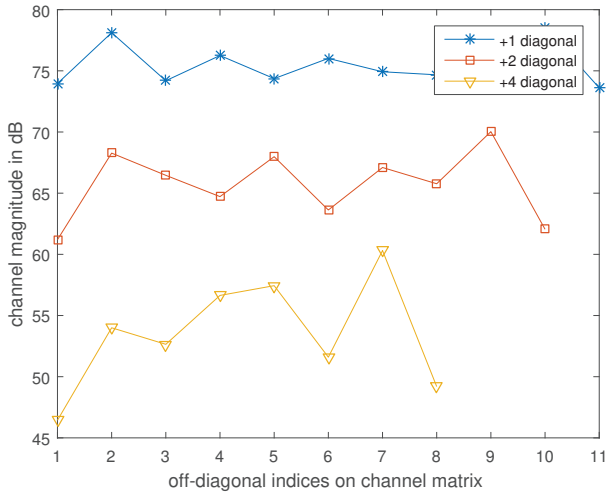

Fig. 4. Variation in channel magnitude for the derived internal channel of row 3 of the antenna array. The different off-diagonals correspond to different distances across the antennas.

Here, we estimate the internal channel and the absolute calibration parameters for the antennas along row 3. Figure 4 shows the magnitude of various off-diagonals of the estimated internal channel obtained from the direct channel estimation method in IV for a single subcarrier. As mentioned in section V, the +1 diagonal corresponds to the internal channel across the neighbouring antennas. Indeed, there is a zig-zag in the channel amplitude as the neighbouring antennas on the same row are not equispaced (see Figure 2). One can also see the channel strength variation as one measures the strength across the +2 diagonal and then, the +4 diagonal. The variation in channel strength across the 12x12 channel matrix can also be seen in Figure 5. The reduction in channel strength with respect to the distance between the antennas is clearly brought out in these figures.

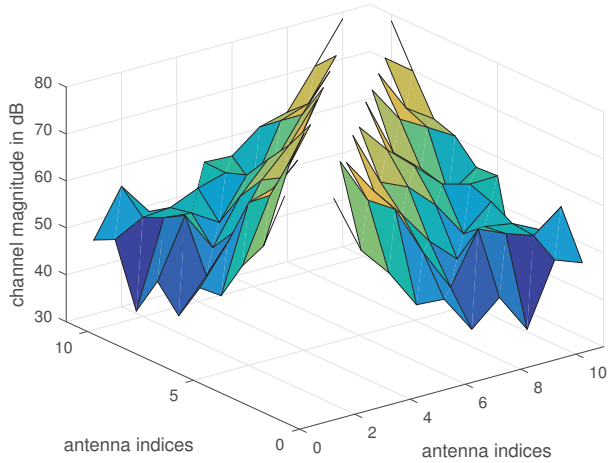

Fig. 5. Surface plot showing the magnitude variation of the estimated internal channel matrix.

Figure 6 compares the variance of **V** obtained with the various approaches (Magnitude only estimation, LoS based phase and linear phase dependency on distance and finally the direct estimation of the internal channel). We assume that the variance of all the elements of **V** is constant. The variance of the elements of **V** is obtained as the overall LSE (Least Square Error) between the received vector and the model divided by the number of equations minus the number of unknowns. For instance, consider the Magnitude only estimation. Let N be the number of antennas in one row of the massive MIMO array (N=12 here). Now, in (1), the total number of equations we have is $N^2 - N$, as the diagonal elements are not available. The number of unknowns are $2N-1$ for the calibration factors and 1 for the unknown parameter γ. Hence, the variance of the elements of **V** may be computed as $\frac{||\text{vec}(\mathbf{H})-(\mathbf{I}*\mathbf{RC})\mathbf{t}||^2}{N^2-N-(2N-1+1)}$. The variance thus obtained may be compared with the channel power in Figure 4 to see the relative level of error. All the estimation methods in the paper are steps in alternating minimization [13] and are hence guaranteed to converge. This behavior is also clearly seen in Figure 6. Furthermore, we can see that the direct channel estimation method is far superior to assuming a parametrized path loss model for C, particularly when the channel phase also has to be estimated.

B. Full Duplex MIMO Internal Channel Rank Profile

From the results of the previous section, the superiority of the direct channel estimation method is clearly established. Hence, for what follows, the channel is assumed to have been estimated with this method. With the channel estimates available, we study the singular values corresponding to some Tx-Rx pairs. For instance, consider the antennas of card 10 as transmit antennas of the Full Duplex (i.e., the antennas (10,x), where $x \in [0, 3]$). Let the antennas (2,0),(4,1),(2,2) and (4,3)

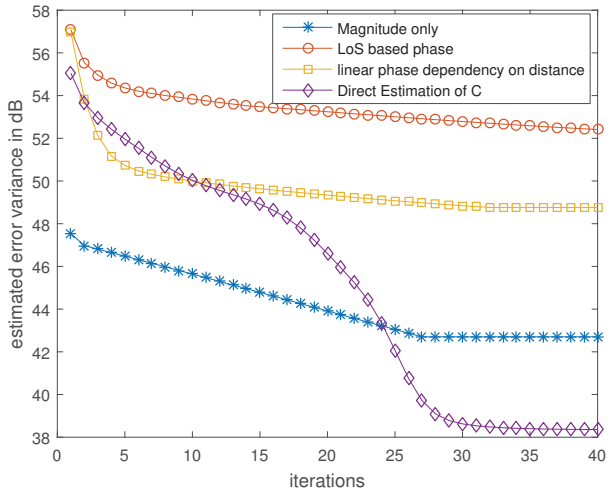

Fig. 6. Plot showing the convergence of error variance for the different approaches.

be the receive antennas of a Full Duplex system. This would form a 4x4 Tx-Rx MIMO channel. Note that the beamforming would be done to null the transmission towards the Rx antennas that see significant power from the Tx antennas, hence in our choice of Tx-Rx pairs, we choose antenna pairs that see significant channel strength between them. Figure 7 shows the singular values of this 4x4 MIMO channel where we see that the strength of the last two singular values is much smaller than the first indicating a low effective rank for the overall channel. The same figure also shows the singular value

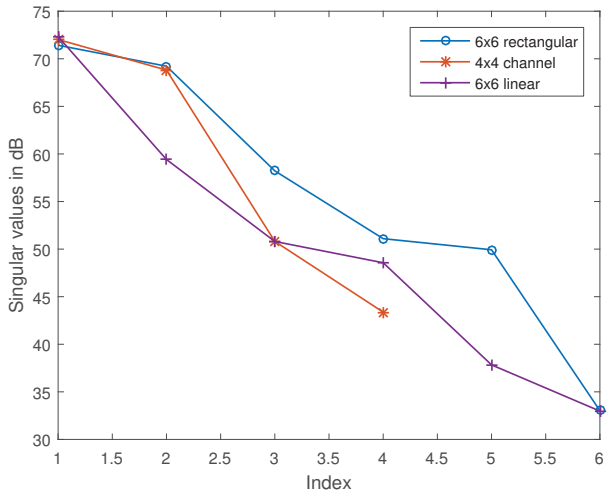

Fig. 7. Variation in singular values for the 4x4 and 6x6 MIMO channels between the Tx and Rx antennas.

profile for a rectangle shaped choice of antennas where Tx is composed of (10,0),(10,1),(2,1),(10,3),(10,2),(2,3) and the Rx comprises (4,1),(4,0),(11,1),(4,3),(4,2),(11,3). Similarly, a linear selection of antennas is also considered where Tx is composed of (10,0),(10,1),(2,1),(2,0),(4,1),(4,0) and the Rx comprises (11,1),(11,0),(8,1),(8,0),(6,1),(6,0). In these scenarios, we observe the last 3 singular values to be much weaker indicating a low channel rank profile.

VII. Conclusion

In this work, we revisit the technique of mitigating the self interference from the Tx to the Rx for a full duplex receiver using multiple antennas. Therefore we extract the internal propagation channel from the estimated digital channel through absolute calibration. To this end, we first propose different methods to estimate the absolute calibration factors. The method of directly estimating the internal propagation channel (section IV) is quite generic and does not require any knowledge of the geometry of the antenna array and is hence very convenient from a practical viewpoint as well. The convergence of the method is also guaranteed. Once the internal channel measurements are completed, the MIMO channel rank profile between different Tx and Rx combinations can be evaluated by observing the singular values. All these measurements have been performed on the Eurecom OAI Massive MIMO antenna array to validate this approach.

Acknowledgments

EURECOM's research is partially supported by its industrial members: ORANGE, BMW, ST Microelectronics, Symantec, SAP, Monaco Telecom, iABG, and by the projects HIGHTS (EU H2020) , DUPLEX (French ANR) and MASS-START (French FUI).

References

[1] GenXComm, ," http://www.edn.com/electronics-blogs/5g-waves/4458607/Startup-promises-to-change-the-wireless-game.

[2] M. Duarte and A. Sabharwal, "Full-duplex wireless communications using off-the-shelf radios: Feasibility and first results," in *Asilomar Conf. on Signals, Systems and Computers*, Nov 2010.

[3] D. Bharadia, E. McMilin, and S. Katti, "Full duplex radios," *SIGCOMM Comput. Commun. Rev.*, vol. 43, Aug. 2013.

[4] E. Tsakalaki, E. Foroozanfard, E. D. Carvalho, and G. F. Pedersen, "A 2-order mimo full-duplex antenna system," in *The 8th European Conf. on Antennas and Propagation (EuCAP)*, Apr. 2014.

[5] E. Foroozanfard, O. Franek, A. Tatomirescu, E. Tsakalaki, E. D. Carvalho, and G. F. Pedersen, "Full-duplex mimo system based on antenna cancellation technique," *Elec. Lett.*, Jul. 2014.

[6] E. Everett, C. Shepard, L. Zhong, and A. Sabharwal, "Softnull: Many-antenna full-duplex wireless via digital beamforming," *IEEE Trans. Wireless Communications*, Dec 2016.

[7] N. Nikaein, R. Knopp, F. Kaltenberger, L. Gauthier, C. Bonnet, D. Nussbaum, and R. Ghaddab, "Demo: OpenAirInterface: an open LTE network in a PC," in *Int'l Conf. Mobile Computing and Networking (MOBICOM),*, Maui, USA, Sept. 2014.

[8] M. Guillaud, D. T. M. Slock, and R. Knopp, "A practical method for wireless channel reciprocity exploitation through relative calibration," in *Proceedings of the Int'l Symp. on Signal Processing and Its Applications (ISSPA).*, Aug. 2005.

[9] D. Inserra and A.M. Tonello, "Performance analysis of a novel antenna array calibration approach for direction finding systems," *European Trans. Telecomms (ETT)*, 2012.

[10] X. Jiang, M. Čirkić, F. Kaltenberger, G. L. Larsson, L. Deneire, and R. Knoppe, "MIMO-TDD reciprocity and hardware imbalances: Experimental results," in *Proc. IEEE Int'l Conf. on Commun. (ICC)*, London, United Kingdom, Jun. 2015.

[11] X. Jiang, A. Decurninge, K. Gopala, F. Kaltenberger, M. Guillaud, and D. Slock, "TDD Reciprocity Calibration in Massive MIMO Systems," *Subm. IEEE Trans. Wireless Comm.*, 2017.

[12] C. G. Khatri and C. R. Rao, "Solutions to some functional equations and their applications to characterization of probability distributions," *Sankhyā: The Indian Journal of Statistics, Series A*, 1968.

[13] P. Stoica and Y. Selen, "Cyclic minimizers, majorization techniques, and the expectation-maximization algorithm: a refresher," *IEEE Sig. Proc. Magazine*, Jan 2004.